Characterization of [Poly(ethylene oxide)] $LiClO–Li_{1.3}Al_{0.3}Ti_{1.7}(PO_4)_3$ Composite Polymer Electrolytes with Poly(ethylene oxide)s of Different Molecular Weights

Yan-Jie Wang,[1] Yi Pan,[1] Li Wang,[1] Ming-Jie Pang,[1] Linshen Chen[2]

[1]*Department of Materials Science and Engineering, Zhejiang University, Hangzhou 310027, People's Republic of China*
[2]*Center of Analysis and Measurement, Zhejiang University, Hangzhou 310027, People's Republic of China*

Received 28 April 2005; accepted 20 December 2005
DOI 10.1002/app.23995
Published online in Wiley InterScience (www.interscience.wiley.com).

ABSTRACT: A group of (PEO)$LiClO_4$–$Li_{1.3}Al_{0.3}Ti_{1.7}(PO_4)_3$ [where PEO is poly(ethylene oxide)] composite polymer electrolyte (CPE) films was prepared by the solution-casting method. In each film, the ethylene oxide/lithium ratio of 8 and the $Li_{1.3}Al_{0.3}Ti_{1.7}(PO_4)_3$ concentration of 15 wt % were fixed, but the number-average molecular weight of PEO was varied (from 5–7 $\times$ 10^4 to 10^6, 2.2–2.7 $\times$ 10^6, 3–4 $\times$ 10^6, 4–5 $\times$ 10^6, and 5.5–6 $\times$ 10^6). Several techniques, including X-ray diffraction, differential scanning calorimetry (DSC), scanning electron microscopy (SEM), and electrical impedance spectroscopy (EIS), were used to characterize the CPE films. $LiClO_4$ had a strong tendency to complex with PEO, but $Li_{1.3}Al_{0.3}Ti_{1.7}(PO_4)_3$ was instead dispersed in the PEO matrix. DSC analysis revealed that the amorphous phase was dominant in the CPE films, although the PEOs before use were quite crystalline. An SEM study showed smooth and homogeneous morphologies for the films with low-molecular-weight PEO and dual-phase characteristics for those with high-molecular-weight PEO. The EIS results indicated that the CPE films were all ionic conductors, and the conducting behavior obeyed the Vogel–Tamman–Fulcher (VTF) equation. The parameters in the VTF equation were obtained and discussed with respect to the PEO molecular weights and the crystallinities of the CPE films. Of all the films, the one with PEO with the smallest number-average molecular weight of 5–7 $\times$ 10^4 had the maximum conductivity, that is, 1.590 $\times$ 10^{-5} S/cm at room temperature and 1.886 $\times$ 10^{-3} S/cm at 373 K. J Appl Polym Sci 102: 1328–1334, 2006

Key words: poly(ethylene oxide); composite polymer electrolyte; ionic conductivity

INTRODUCTION

In contrast to liquid electrolytes in lithium-ion batteries, solid electrolytes have attracted much attention because of their advantages over liquid electrolytes, such as ease of fabrication, low electrolyte leakage, safety, and reliability in batteries.[1–4] An ideal electrolyte for solid-state lithium batteries should have not only high lithium-ion conductivity and a large transport number but also a rubbery mechanical performance to accommodate electrode dimension changes during charging and discharging. With such expectations, poly(ethylene oxide) (PEO) doped with sodium salts was suggested earlier by Wright and coworkers[5,6] and was later recognized by Armand et al.[7] as potentially applicable to high-specific-energy batteries and other electrochemical devices. PEO and other polymers, such as polyacrylonitrile, poly(methyl methacrylate), and poly(vinylidene fluoride), which can form ionic complexes with metal salts of low lattice energy, particularly lithium salts,[8] have been used as polymer matrices for solid polymer electrolytes (SPEs). Moreover, lithium-ion transport mainly takes place in the amorphous phase, and the conductivity in the amorphous phases is 2–3 orders of magnitude higher than that in crystalline phase in SPEs.[9,10] Most research efforts therefore have been dedicated to obtaining SPE films containing large amounts and stable amorphous phases to obtain good flexibility for the polymer chains, which favors ion transport.

Ceramic powders, such as Al_2O_3, SiO_2, and Li_3N, can be added as fillers to improve the ionic conductivity (σ) and preserve the mechanical strength and stability of the electrode/electrolyte interface.[11–13] Instead of nonconducting oxides, fast ionic conductors, such as $Li_{1.4}Al_{0.4}Ge_{1.7}(PO_4)_3$ and $14Li_2O–9Al_2O_3–38TiO_2–39P_2O_5$, have been used as fillers in PEO-based composite polymer electrolyte (CPE) films, and their positive effects on both the mechanical properties and σ were reported by Leo and coworkers[14,15] and Zhang et al.[16] Recently, we reported the $Li_{1.3}Al_{0.3}Ti_{1.7}(PO_4)_3$ filler effect on (PEO)$LiClO_4$ SPE.[17] (PEO)$LiClO_4$–$Li_{1.3}Al_{0.3}Ti_{1.7}(PO_4)_3$ CPE films with an overall ethylene

Correspondence to: Y. Pan (yipan@zju.edu.cn).

oxide (EO)/Li ratio of 8 and 15 wt % $Li_{1.3}Al_{0.3}Ti_{1.7}(PO_4)_3$ had optimum σ values, that is, 1.387×10^{-5} S/cm at room temperature and 1.378×10^{-5} S/cm at 373 K.[17] This article extends the study to the investigation of (PEO)$LiClO_4$–$Li_{1.3}Al_{0.3}Ti_{1.7}(PO_4)_3$ CPE films with an overall EO/Li ratio of 8 and 15 wt % $Li_{1.3}Al_{0.3}Ti_{1.7}(PO_4)_3$ but PEOs of different molecular weights. The film preparation, phase composition, thermal behavior, morphologies, and σ values are studied. The effects of the PEO molecular weight on all these factors are discussed.

EXPERIMENTAL

Synthesis of the materials

The preparation of $Li_{1.3}Al_{0.3}Ti_{1.7}(PO_4)_3$ from the raw materials Li_2CO_3, Al_2O_3, TiO_2, and $(NH_4)_2HPO_4$ was based on the method described by Aono et al.[18] Before use, the $Li_{1.3}Al_{0.3}Ti_{1.7}(PO_4)_3$ ceramic, confirmed by X-ray diffraction (XRD), was proved to be an air-stable, lithium-ion conductor of about 10^{-4} S/cm at room temperature. The ceramic was crushed and milled with agate balls in alcohol for 90 h to attain the particle size distribution shown in Figure 1, which was thought satisfactory for incorporation into the PEO matrix for this study.[15] The fine powder was dried *in vacuo* at 120°C for 48 h to get rid of all possibly attached water molecules.

PEO polymers with number-average molecular weight (M_n) values of 5–7 $\times 10^4$ (M_1), 10^6 (M_2), 2.2–2.7 $\times 10^6$ (M_3), 3–4 $\times 10^6$ (M_4), 4–5 $\times 10^6$ (M_5), and 5.5–6 $\times 10^6$ (M_6), supplied by Aldrich Chemical Co. (Shanghai, China), were solely dried *in vacuo* at 50°C for 48 h right before the preparation of the CPE films. Acetonitrile (reagent-grade), used as the solvent, was doubly distilled and stored over 4-Å molecular sieves before use. Anhydrous $LiClO_4$, provided by Zhangjianggang Guotai–Huarong New Chemical Materials Co., Ltd. (China), was used as the main lithium-ion contributor in the CPE after it was dried at 120°C for 24 h.

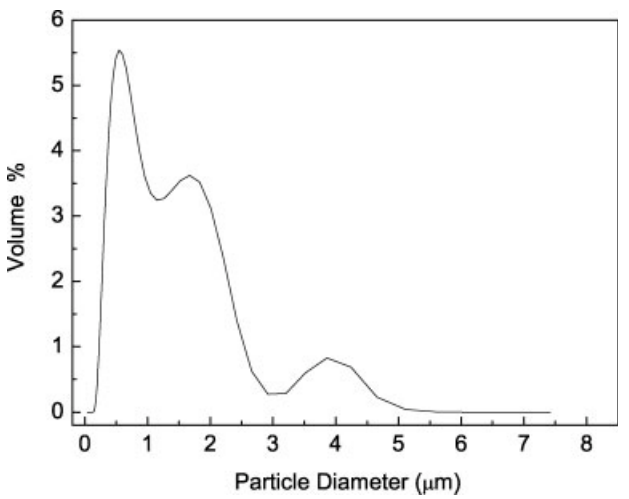

Figure 1 Particle size distribution of the $Li_{1.3}Al_{0.3}Ti_{1.7}(PO_4)_3$ salt after ball milling.

$Li_{1.3}Al_{0.3}Ti_{1.7}(PO_4)_3$, $LiClO_4$, and one of the PEO powders were appropriately weighed to guarantee a $Li_{1.3}Al_{0.3}Ti_{1.7}(PO_4)_3$ concentration of 15 wt % and an EO/Li ratio of 8 in each CPE system, and then they were added to the previously treated acetonitrile in a beaker; this was followed by stirring at 50–70°C until a homogeneous suspension was formed. The suspension was cast onto a Teflon plate and then slowly dried at room temperature. The final films, with a thickness of 150–300 μm, were yielded and dried at 45–50°C *in vacuo* for 24 h before the measurements. Corresponding to each PEO used, the films were labeled CPE(1), CPE(2), CPE(3), CPE(4), CPE(5), and CPE(6).

Characterization

The phases of the various pure PEOs and CPE films were analyzed with XRD (D8 Advance AXS, Bruker GMBH, Germany; 30 kV, Cu Kα radiation with a step width of 0.02°) at room temperature. The thermographs, from −100 to 100°C, of the films were obtained with differential scanning calorimetry (DSC; Q100, Delaware) with a liquid-nitrogen-cooled heating element. Each sample to be analyzed by DSC was sealed in an aluminum pan, heated from 25 to 100°C, and then cooled to −100°C; measuring began with heating again to 100°C at a heating rate of 10°C/min. Morphology observations of the films were carried out with scanning electron microscopy (SEM; S-570, Hitachi, Japan). Thin electrolyte films prepared by a solution-casting technique were mounted onto 1-cm-diameter aluminum plates. The samples were sputter-graphite-coated (20 nm). The surface morphology of all specimens was examined at a working voltage of 25 kV. σ was determined with electrical impedance spectroscopy (EIS) at different temperatures. The CPE film samples were sandwiched between stainless steel blocking electrodes and placed in a temperature-controlled furnace. The impedance of the films was measured with a frequency response analyzer (model 1255, FRA Solartron, UK) and a Solartron model 1287 electrochemical interface over the frequency range of 1 Hz to 1 MHz.

RESULTS AND DISCUSSION

Phases

Figure 2(A,B) shows the XRD patterns of various pure PEOs, two lithium salts, and CPE films. In Figure 2(A), two strong peaks at 2θ values of 19.5 and 23.5° and minor peaks at 15.08, 26.24, 26.94, 35.3, 36.26, and

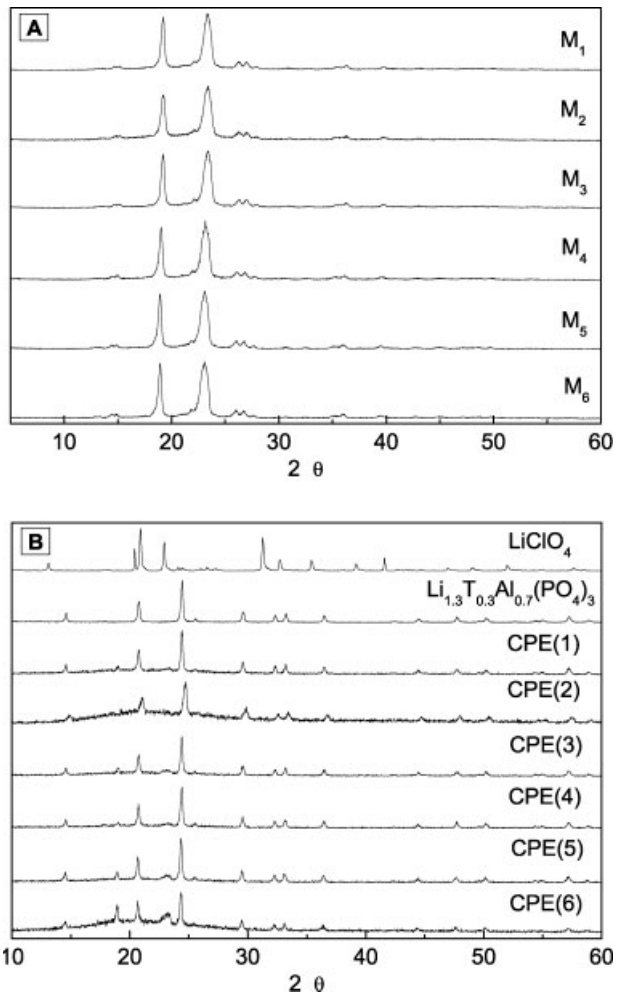

Figure 2 XRD patterns at room temperature of (A) pure PEOs with different molecular weights and (B) $LiClO_4$, $Li_{1.3}Al_{0.3}Ti_{1.7}(PO_4)_3$, and different CPE films with a fixed EO/Li ratio of 8 and 15 wt % $Li_{1.3}Al_{0.3}Ti_{1.7}(PO_4)_3$.

39.68° can be found for all the PEOs, suggesting that all the PEOs were intrinsically crystalline polymers with high crystallinity. Additionally, the X-ray traces of the CPE films in Figure 2(B) explicitly show that $LiClO_4$ characteristic peaks at 13.16, 20.38, 20.88, 22.9, 31.24, 39.14, 41.56, 47, 49.04, and 52.04° all disappear and that $Li_{1.3}Al_{0.3}Ti_{1.7}(PO_4)_3$ characteristic peaks at 14.54, 20.76, 24.4, 25.54, 29.52, 32.36, 33.26, 36.46, 44.52, 47.72, 50.26, 55.06, 57.26, and 58.9° remain, indicating that $LiClO_4$ dissolved, that is, complexed with PEO and that $Li_{1.3}Al_{0.3}Ti_{1.7}(PO_4)_3$ was mechanically dispersed rather than complexed in PEO; the previous finding is in agreement with the work done by Robitaille and Fauteux[19] and Valllee et al.[20] Meanwhile, the intensities of two main peaks of pure PEO in the CPE films slightly decreased with a decrease in the molecular weight of PEO, suggesting that the degree of crystallinity (χ_c) of PEO in the CPE films was low when the molecular weight was low. This is further discussed in the following section.

Crystallinity

The DSC thermograms obtained from pure PEOs and CPE films are drawn in Figure 3(A,B), respectively. For pure PEOs, only melting peaks and consequently melting temperatures (T_m's) are identifiable. For CPE films, however, the glass-transition temperatures (T_g's) can be determined, but the melting peaks do not show up except for CPE(5) and CPE(6). The possibly defined T_g and T_m values are marked in Figure 3 and summarized in Table I. It is suggested that the addition of two lithium salts inhibited the crystallization of PEO in the CPE films so that low-molecular-weight CPE(1) to CPE(4) did not give melting peaks and high-molecular-weight CPE(5) and CPE(6) gave faded melting peaks. The inhibition of crystallization may favor σ for lithium because ionic transport only takes place in the amorphous region of CPEs.[9,10] On the basis of these curves, their χ_c values were calculated with the following equations:

$$\chi_c(\text{CPE}) = \frac{\Delta H_{m,\text{CPE}}}{\Delta H^0_{m,\text{CPE}}} \quad (1)$$

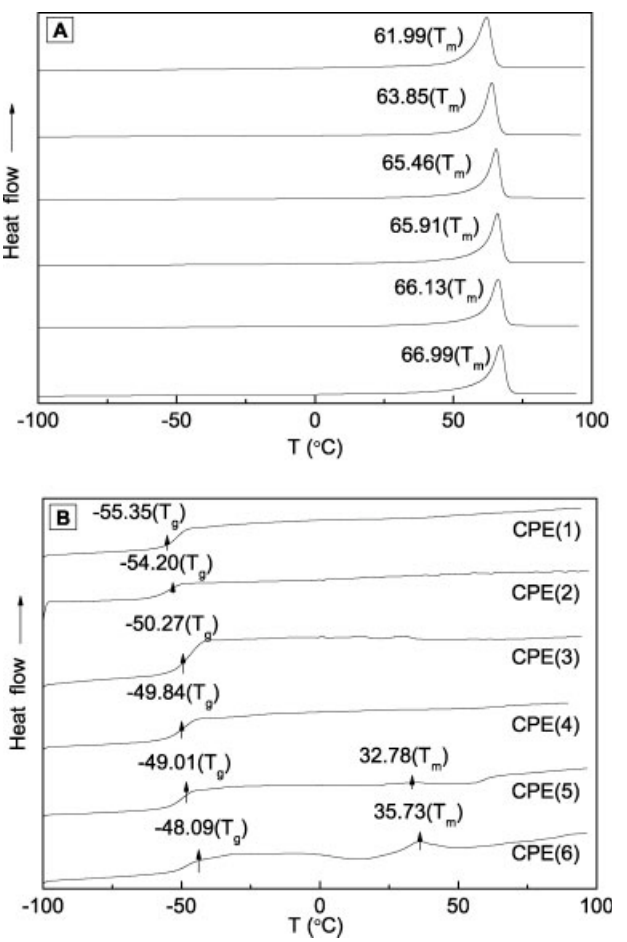

Figure 3 DSC curves of (A) PEOs with different molecular weights and (B) CPE films made from these PEOs with a fixed EO/Li ratio of 8 and 15 wt % $Li_{1.3}Al_{0.3}Ti_{1.7}(PO_4)_3$.

TABLE I
Thermal Properties of PEOs with Different Molecular Weights and CPE Films

PEO or CPE	T_g (°C)	T_m (°C)	ΔH_m (J/g)	ΔH^0_{PEO} (J/g)	χ_c (%)
M_1	—	61.99	129.3	182.52	46.92
M_2	—	63.85	129.7	188.00	68.99
M_3	—	65.46	129.8	192.74	67.34
M_4	—	65.91	131.5	194.07	67.76
M_5	—	66.13	136.1	194.71	69.90
M_6	—	66.99	145.0	197.25	73.51
CPE(1)	−55.35	—	—	182.52	—
CPE(2)	−54.20	—	—	188.00	—
CPE(3)	−50.27	—	—	192.74	—
CPE(4)	−49.84	—	—	194.07	—
CPE(5)	−49.01	32.78	0.827	194.71	0.425
CPE(6)	−48.09	35.73	4.450	197.25	2.256

$$\chi_c(\text{PEO}) = \frac{\Delta H_{m,\text{PEO}}}{\Delta H^0_{m,\text{PEO}}} \quad (2)$$

where $\Delta H_{m,\text{CPE}}$ and $\Delta H_{m,\text{PEO}}$ are the apparent melting enthalpies per gram of CPE and PEO present in the CPE, respectively, and ΔH^0_{PEO} is the heat of melting per gram of 100% crystalline PEO. T_g and T_m of the pure PEOs and CPE films, as well as their ΔH^0_{PEO}, $\Delta H_{m,\text{PEO}}$,[21,22] and χ_c values, are also summarized in Table I. The χ_c values of the pure PEOs fluctuated around 63–74%, but those of CPE were mostly 0 [0.425 and 2.26% for CPE(5) and CPE(6), respectively]. Besides that, the T_m values for CPE(5) and CPE(6), the only ones with well-defined T_m values, were much lower than that of pure PEO.

Morphology

The surfaces of all CPE films, which were only PEO envelopes, were observed in SEM, but only the surface morphologies of CPE(1) and CPE(6) are shown in Figure 4(a,b), representing completely amorphous and partially crystalline PEO in the films. The surface of CPE(1) was smooth, but CPE(6) exhibited dual-phase characteristics, confirming the DSC results; that is, high-molecular-weight PEO in a CPE film is partially crystalline.

Electrical impedance spectra

The electrical impedance spectra of CPE films were measured at various temperatures. The room-temperature impedance spectra of the CPE films with different PEO molecular weights are shown in Figure 5(B). The use of alternating-current techniques for classical electrochemical measurements has been reviewed by Armstrong et al.,[23] but the problem of surface roughness is ignored. The spectra of the films, which are situated between two stainless steel electrodes, all consist of a depressed semicircle in a high-frequency range and a straight line in a low-frequency range. The former represents the ionic impedance of the polymer electrolyte, and the straight line is from the stainless steel electrodes and can be attributed to ion diffusion in the polymer electrolyte. The semicircle part of each spectrum can be molded with an equivalent circuit, as shown in Figure 5(A). The physical meanings of the elements in this assumed equivalent circuit are as follows: R_b and C_1 represent the bulk resistance and geometrical capacitance of the electrolyte, respectively, and R_w represents the Warburg impedance. The equivalent circuit is commonly used in the analysis of impedance spectroscopy because it is simple and can provide a complete picture of the system.[24] With this equivalent circuit, R_b, C_1, and R_w can be estimated by the super-

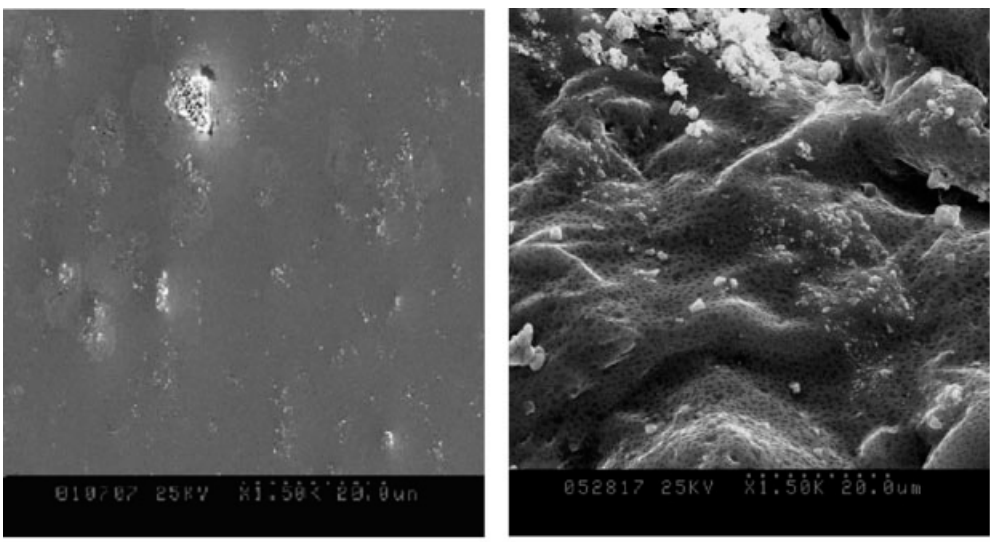

(a) (b)

Figure 4 SEM micrographs of CPE films with PEOs of different molecular weights: (a) CPE(1) and (b) CPE(6).

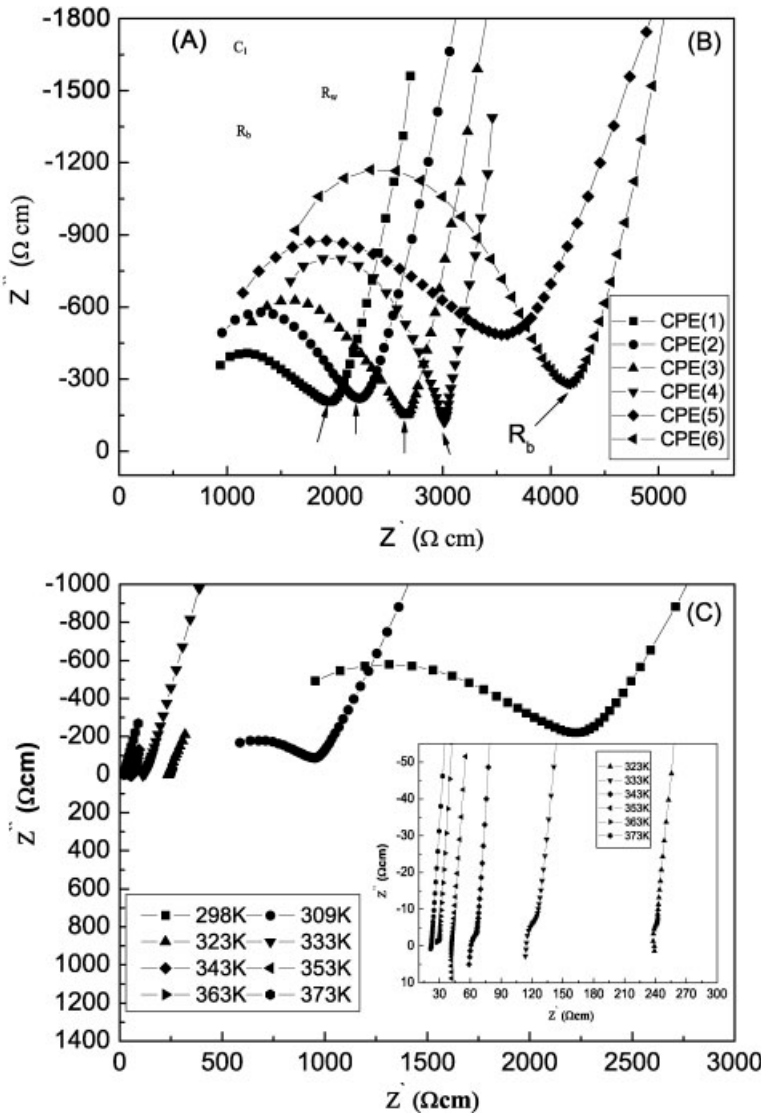

Figure 5 (A) Equivalent circuit for the simulation of impedance spectra, (B) impedance spectra of CPE films at room temperature with different molecular weights, and (C) impedance spectra of CPE(2) films at various temperatures.

imposition of the best fit to the measured spectrum, as shown in Figure 5(B).

The impedance spectra of the CPE(2) films at different temperatures are shown in Figure 5(C). At higher temperatures (≥323 K), the semicircle shrinks as a result of its shift to higher frequencies due to the decrease in the ionic resistance of the polymer electrolyte. In this case, R_b is determined with the intercepting point of the inclined line with the Z' axis.

σ is calculated as follows:

$$\sigma = \frac{d}{R_b A} \tag{3}$$

where d and A represent the thickness and area of the sample, respectively. The conductivity of CPE

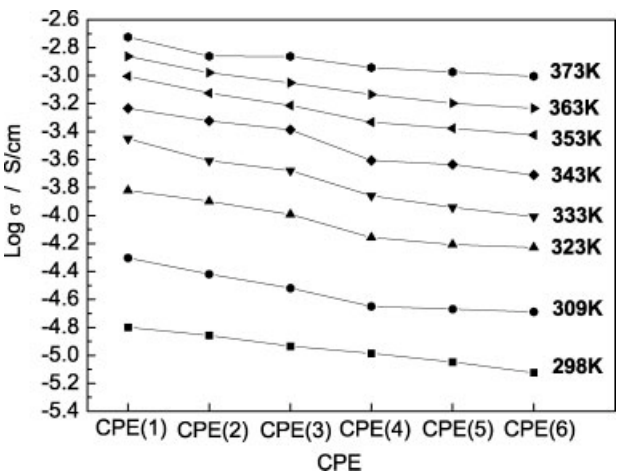

Figure 6 σ as a function of the molecular weight for CPE films at various temperatures.

films with a fixed EO/Li ratio of 8 and 15 wt % $Li_{1.3}Al_{0.3}Ti_{1.7}(PO_4)_3$ at different temperatures is plotted against the PEO molecular weight in Figure 6. For the CPE films, when the temperature increased, σ mainly increased because the crystallinity was severely damaged after the addition of $Li_{1.3}Al_{0.3}Ti_{1.7}(PO_4)_3$ and $LiClO_4$ to PEO. After the temperature increased above T_m, the disappearance of the crystalline phase and consequently the increase in the amorphous regions in the CPE films made σ high. For the CPE(1) to CPE(4) films, the increase in σ with increasing temperature was attributed to higher and higher ionic mobility in the amorphous phase because there was no T_m, as DSC studies showed. Additionally, σ of the films was low when the molecular weight of PEO in the films was high. CPE(1), with the lowest molecular weight, had the highest conductivity, that is, 1.590×10^{-5} S/cm at room temperature and 1.886×10^{-3} S/cm at 373 K.

To further study the temperature dependence of the conductivity, two plots are drawn in Figure 7(A,B). One is log σ versus $1000/T$, and the other is log $\sigma T^{-0.5}$ versus $1000/T$, corresponding to the

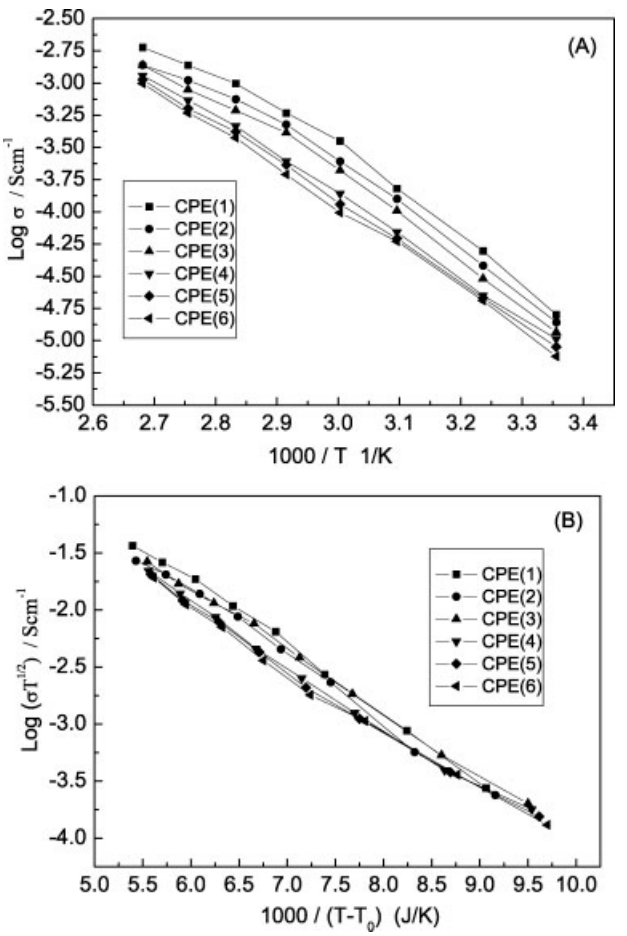

Figure 7 Temperature-dependent conductivity of CPE films with a fixed EO/Li ratio of 8, PEOs of various molecular weights, and 15 wt % $Li_{1.3}Al_{0.3}Ti_{1.7}(PO_4)_3$.

TABLE II
Fitted Parameters Obtained from Conductivity Data for the CPE Films

PEO	T_0 (K)	A (S/cm $K^{1/2}$)	E_a (eV)
M_1	187.65	61.671	0.135
M_2	188.8	40.280	0.132
M_3	192.73	28.278	0.125
M_4	193.16	18.853	0.123
M_5	193.99	16.280	0.122
M_6	194.91	14.410	0.121

Arrhenius relationship and Vogel–Tamman–Fulcher (VTF) equation,[25–27] that is, eq. (4), respectively:

$$\sigma = AT^{-1/2} \exp[-E_a/k_B(T - T_0)] \quad (4)$$

where T is the absolute temperature, A is the pre-exponential factor, E_a is the pseudo-activation energy, k_B is the Boltzmann constant, and T_0 is a reference temperature that is usually 30–50 K lower than T_g.[28–30] The VTF equation fits better than the Arrhenius relationship and is thus adopted to describe the ionic conduction behavior of the CPE films in this study.

By fitting the conductivity data to eq. (4), we obtained T_0, A, and E_a, which are summarized in Table II. The VTF equation, applied to polymer electrolytes, was discussed by Berthier et al.[31] A is proportional to the number of ionic charge carriers. E_a reflects the energy characteristics, combining various ion–polymer and ion–ion interactions, and is controlled by many factors, such as the lattice energy of the salt, complexation degree, concentration, crystallinity, and dielectric constant. In Table II, A decreases and T_0 increases, whereas E_a does not change much, with the increasing molecular weight of PEO. This suggests that the number of ionic charge carriers is reduced, the PEO matrix becomes less flexible, and the ion–polymer and ion–ion interactions are basically the same with the increasing PEO molecular weight.

CONCLUSIONS

As CPEs, (PEO)$LiClO_4$–$Li_{1.3}Al_{0.3}Ti_{1.7}(PO_4)_3$ films [15 wt % $Li_{1.3}Al_{0.3}Ti_{1.7}(PO_4)_3$ and EO/Li = 8] with M_n values of PEO of 5–7 $\times 10^4$, 10^6, 2.2–2.7 $\times 10^6$, 3–4 $\times 10^6$, 4–5 $\times 10^6$, and 5.5–6 $\times 10^6$ were successfully prepared with a solution-casting technique. An XRD study suggested that the PEO matrix was largely complexed with $LiClO_4$ rather than $Li_{1.3}Al_{0.3}Ti_{1.7}(PO_4)_3$. DSC results indicated that amorphous PEO with $LiClO_4$ complexes dominated in these CPE films after the addition of $LiClO_4$ and $Li_{1.3}Al_{0.3}Ti_{1.7}(PO_4)_3$, although the PEO samples were highly crystalline. The PEO-enveloped surfaces observed in SEM exhibited smooth and homogeneous morphologies for the

films with relatively low-molecular-weight PEO and dual-phase (amorphous and crystalline) characteristics for the films with high-molecular-weight PEO. An analysis of the EIS evidence showed that σ of the CPE films was low when the molecular weight of PEO in the films was high. The conductivity of the film with PEO of $M_n = 5–7 \times 10^4$, the lowest in this study, was 1.590×10^{-5} S/cm at room temperature and 1.886×10^{-3} S/cm at 373 K. The ionic conducting behavior of the CPE films obeyed the VTF equation:

$$\sigma = AT^{-1/2} \exp[-E_a/k_B(T - T_0)]$$

A decreased and T_0 increased, whereas E_a did not change much, with the increasing molecular weight of PEO.

References

1. Jacob, M. M. E.; Hackett, E.; Giannelis, E. P. J Mater Chem 2003, 13, 1.
2. Bruce, P. G. Electrochim Acta 1995, 40, 2077.
3. Armand, M.; Sanchez, J. Y.; Gauthier, M.; Choquette, Y. In Electrochemistry of Novel Materials; Lipkowski, J.; Ross, P. N., Eds.; VCH: New York, 1994; p 65.
4. Quartarone, E.; Mustarelli, P.; Magistris, A. Solid State Ionics 1998, 110, 1.
5. Fenton, D. E.; Parker, J. M.; Wright, P. V. Polymer 1973, 14, 589.
6. Wright, P. V. Br Polym J 1975, 7, 319.
7. Armand, M. B.; Chabagno, J. M.; Duclot, M. In Fast Ion Transport in Solids; Vashishta, P.; Mundy, J. N.; Shenoy, G. K., Eds.; Elsevier: New York, 1979; p 131.
8. Gray, F. M. Solid Polymer Electrolytes; VCH: New York, 1991.
9. Berthier, C.; Gorecki, W.; Minier, M.; Armand, M. B.; Chabagno, J. M.; Rigaud, P. Solid State Ionics 1983, 11, 91.
10. Stainer, M.; Hardy, L. C.; Whitmore, D. H.; Shriver, D. F. J Electrochem Soc 1984, 181, 784.
11. Tambelli, C. C.; Bloise, A. C.; Rosario, A. V.; Pereira, E. C.; Magon, C. J.; Donoso, J. P. Electrochim Acta 2002, 17, 1677.
12. Capiglia, C.; Mustarelli, P.; Quartarone, E.; Tomasi, C.; Magistris, A. Solid State Ionics 1999, 118, 73.
13. Skaarup, S.; West, K.; Julian, P. M.; Thomas, D. M. Solid State Ionics 1990, 40, 1021.
14. Leo, C. J.; Subba Rao, G. V.; Chowdari, B. V. R. Solid State Ionics 2002, 148, 159.
15. Leo, C. J.; Thakur, A. K.; Subba Rao, G. V.; Chowdari, B. V. R. J Power Sources 2003, 115, 295.
16. Zhang, X.-W.; Wang, C. S.; Appleby, A. J.; Little, F. E. J Power Sources 2002, 112, 209.
17. Wang, Y.-J.; Pan, Y. J Polym Sci Part B: Polym Phys 2005, 43, 743.
18. Aono, H.; Sugimoto, E.; Sadaoka, Y.; Imanaka, N.; Adachi, G. Y. J Electrochem Soc 1990, 137, 1023.
19. Robitaille, C. D.; Fauteux, D. J Electrochem Soc 1986, 133, 315.
20. Valllee, A.; Besner, S.; Prud Homme, J. Electrochim Acta 1992, 37, 1579.
21. Cimmino, S. Makromol Chem 1990, 19, 2447.
22. Rocco, A. M.; Da Fonseca, C. P.; Pereira, R. P. Polymer 2002, 43, 3601.
23. Armstrong, R. D.; Bell, M. F.; Metcalfe, A. A. Electrochim Acta 1976, 6, 98.
24. Han, D. G.; Choi, G. M. Solid State Ionics 1998, 106, 71.
25. Vogel, H. Phys Z 1922, 22, 645.
26. Tamman, G.; Hesse, W. Anorg Z Allg Chem 1956, 156, 245.
27. Fulcher, G. S. J Am Ceram Soc 1925, 8, 339.
28. Li, X.; Hsu, S. L. J Polym Sci Polym Phys Ed 1984, 22, 1331.
29. Bruce, P. G.; Vincent, C. A. J Chem Soc Faraday Trans 1993, 89, 3187.
30. Albinsson, I.; Mellander, B.-E.; Stevens, J. R. J Chem Phys 1992, 96, 681.
31. Berthier, C.; Gorecki, W.; Minier, M.; Armand, M. B.; Chabagno, J. M.; Rigaud, P. Solid State Ionics 1983, 11, 91.